Int. J. Electrochem. Sci., 5 **(2010)** 1837 - 1846

International Journal of
ELECTROCHEMICAL
SCIENCE
www.electrochemsci.org

Fabrication of Electrochemically Deposited Microelectrodes for Microfluidic MEMS Applications

Abdulilah Dawoud Bani-Yaseen

Department of Chemistry, Faculty of Science
Taibah University, Al-Madinah Al-Munawarah P.O. Box 30002, KSA
*E-mail: aayaseen@yahoo.com

Received: 22 September 2010 / *Accepted:* 15 October 2010 / *Published:* 1 December 2010

In this paper the electrochemical deposition of three metals, namely gold, palladium, and platinum over gold microelectrode seeded by titanium thin layer in microfluidic channel has been investigated. Modified microelectrodes were characterized with cyclic voltammetry, scanning electron microscope (SEM), and surface profilometry. Cyclic voltammograms data of all modified electrodes, namely aurized, palladized, and platinized microelectrodes exhibited their characteristic oxygen deposition peak (aurized) and hydrogen adsorption peaks (platinized and palladized). The real surface area, or roughness factor, and height of each microelectrode were measured after every single deposition patch. Obtained results revealed that aurized and palladized microelectrodes reached their maximum value of surface area after approximately 10 minutes of electrochemical deposition, whereas platinized microelectrodes exhibited gradual increase in surface area even after long time of electrochemical deposition. Using aurized microelectrodes for chronoamperometric analysis of dopamine exhibited similar behavior. Furthermore, SEM and surface profilometry results revealed that the process of electrochemical deposition of microelectrode in microfluidic channels is influenced by the edge effect, where the deposition process proceeds mainly at the kinks along the step (~ 21 nm high) of the microelectrodes.

Keywords: Microelectrodes, electrochemical deposition, surface roughness, chronoamperometric analysis, microfluidic MEMS.

1. INTRODUCTION

Tremendous amount of efforts have been exerted in developing miniaturized microfluidic systems since the introduction of this concept in the early 1990s [1,3]. In particular, integrated microfluidic systems has recently gained a great amount of attention because of their potential portability in addition to their prospective broad range of applications, such as biomedical diagnostics [4-7], genomic and proteomics analyses [8-12], drug discovery and delivery [13-15], and

environmental investigations [16-19]. However, various fabrication techniques that have been developed in the landscape of micro electronics and semi-conductors industries in combination with well-established conventional analytical techniques have prompted the efforts toward designing and fabricating innovative class of microfluidic systems defined as microfluidic micro-electro-mechanical-systems (MEMS), i.e. microfluidic MEMS.

Typically, a microfluidic MEMS comprise sets of microchannels and microelectrodes, where the latter are designed in a pattern that can control the flow of a fluid selectively and sensitively inside the microchannels. Practically, two separate substrates are needed to generate a functional microfluidic MEMS, where the microchannels that are encompassed on the first substrate are sealed by bonding to the second substrate where microelectrodes are located. It is noteworthy mentioning that such bonding between the two substrates requires very thin films of microelectrodes, usually few nanometers thick. However, this bonding process is practically challenging when thick electrodes are needed, bonding is retarded by thick microelectrodes. In addition, bonding two hard materials together, such as glass to glass bonding, is another practical challenge in the presence of microelectrodes, which usually has limited rate of success. Interestingly, electrochemical deposition provides sufficient remedy in this practical challenge, where thick electrodes are generated after performing the bonding process, which in turn is facilitated via fabricating the microchannels on soft polymeric material, such as PDMS, whereas microelectrodes are fabricated on hard materials, such as glass. Recently, various kinds of materials have been utilized for fabricating microfluidic systems that are comprised in these types of microfluidic MEMS, this includes PDMS [20-22], glass and silicon wafers [23-25], SU-8 photoresists [26,27]. However, using PDMS has superior advantages, namely its softness and easiness of fabrication, over other hard materials such as glass. Moreover, PDMS exhibits surface characteristics that are comparable to glass upon utilizing electroosmotic flow (EOF) as the driving force for flow of liquids, aqueous solutions in particular, inside the microchannels. On the other hand, electrochemical deposition has recently been progressively utilized for generating thick electrodes integrated within microfluidic MEMS. Furthermore, electrochemical deposition offers straightforward procedure for fabricating microelectrodes that are made of various kinds of metals [28-32]. Nevertheless, inserting thick microelectrodes inside a microchannel does not only applicable for chip-based electrophoresis, but also can be utilized for gaining insights concerning the driving force and mechanism of EOF inside a microchannel [28-30]. Several reports ahs recently appeared in the literature dealing with the technique of electrochemical deposition for incorporating thick microelectrodes or pillars inside microchannels [20, 33-35]. In our previous work we reported fabrication and potential application of various integrated microfluidic systems [33-35] In particular, electrochemical deposition was utilized for incorporating palladium de-coupler within an integrated microfluidic systems functioning based on electrophoretic separation for the analyses of various analytes of biomedical importance, such as DNA adducts [20].

Although designing and fabricating novel microfluidic MEMS is occurring progressively in notable rate, particularly incorporating pillar and thick microelectrodes inside a microchannel using electrochemical deposition, there is still a necessity for gaining knowledge regarding the potential geometric profile of extra thick microelectrodes [36-39]. The goal of this work is to gain insights regarding surface profile of integrated microelectrodes fabricated via electrochemical deposition inside

a microfluidic channel. Electrochemical deposition of three metals, namely gold, palladium, and platinum, over a long period of deposition time is investigated, where a square pulse potential signal is used to stimulate the deposition process. Geometric profiles of the microelectrodes are characterized using scanning electron microscope (SEM), cyclic voltammetry, and surface profilometry.

2. EXPERIMENTAL

2.1. Materials

Sodium tetrachloroaurate (III). $2H_2O$ ($NaAuCl_4$. $2H_2O$), potassium hexachloropalladate (IV) (K_2PdCl_6), potassium hexachloroplatinate (IV) (K_2PtCl_6), potassium, and potassium iodine were purchased from Sigma-Aldrich (USA). Photoresists and developing solution, poly dimethylsiloxane (PDMS), microscopic slide, and silicon wafers were supplied by Microchem Co., Dow Corning, Fisher Scientific , and UniversityWafer Co., respectively.

2.2. Apparatus and measurements

All electrochemical measurements including electrochemical deposition were performed with typical three-electrode configuration using PCl4-FAS2potentiostat (Gamry Instruments, Warminster, PA, USA). SEM imaging was performed using JEOL-5910lv SEM (Japan Electron Optics Laboratory) with conventional secondary electron imaging; no special coating or treatment was applied to the specimens. Surface profilometry was conducted employing Dektak (IIA) profilometer. Cyclic voltammograms were collected in 50 mM of HCL_4 prepared in ultrapure water ((18 MΩ cm, Millipore) at scanning rate of 50 $mV.s^{-1}$.

2.3. Microfluidic and microelectrodes fabrication

Detailed procedure for fabrication the microfluidic system has been published previously [20,30]. In brief, the PDMS slabs were fabricated employing a combination of techniques, including soft lithography, photolithography, and molding. Typically, a mold of SU-8 photoresist comprised on silicon wafer with microchannel pattern was initially fabricated; then a premixed mixture of PDMS and curing agent was poured over the mold and set for curing at 60 °C for one hour. After curing, the PDMS slabs were peeled of the mold gently, and then access to the microchannels was generated through punched holes on the PDMS. On the other hand, the microelectrodes array was comprised on microscopic slides, where these microelectrodes are made of gold (20 nm) pre-seeded with titanium (1 nm). A combination of photolithography and chemical wet etching was applied to formulate the microelectrodes according to the desired pattern (See Figure 1). The microelectrodes array consists of 10 microelectrodes with width and spacing between them of 50 μm (Figure 1, Inset I), and two 200 μm wide electrodes, were the 10-electrode array and two wide microelectrodes are located inside the microchannel reservoir A, respectively. The whole system was assembled by permanently bonding the

PDMS slab to the microelectrodes array after 1 min of plasma treatment. The depth and width of the microchannel were 50 and 75 μm, respectively, whereas the length, effective length between reservoirs A and B, was approximately 2 cm.

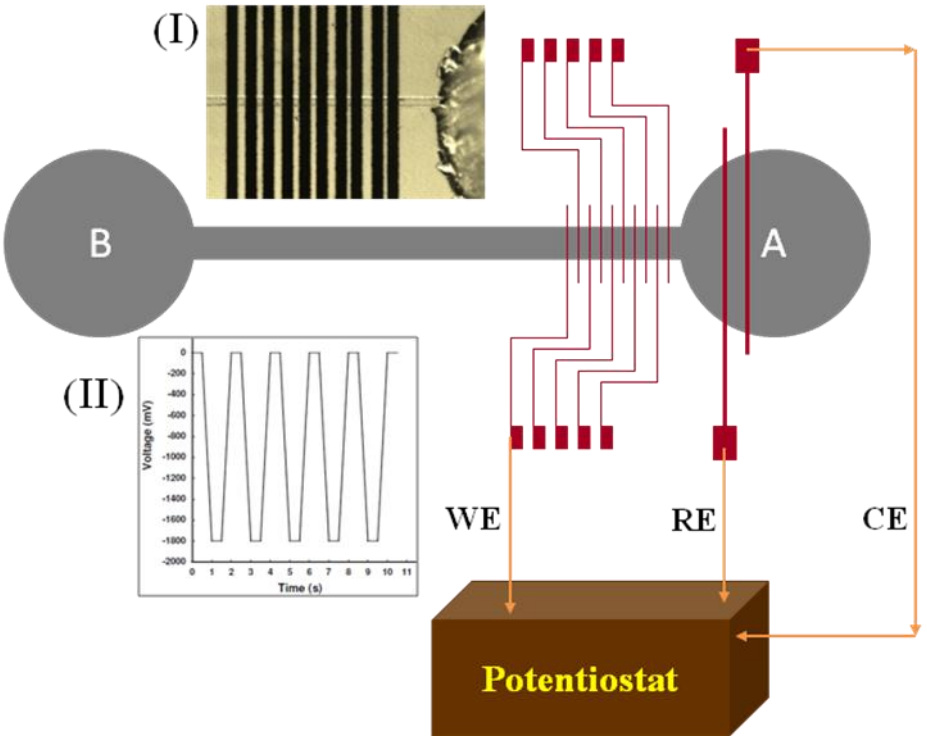

Figure 1. Schematic of experimental setup for electrodepositing metallic nanoparticles on the surface of the microelectrodes inside a microfluidic channel. Insets: (A) Real image for the microfluidic channel at the microelectrodes array region, (B) Potential pulse signal applied to the working electrode for electrochemical deposition.

2.4. Electrochemical deposition

A schematic representation for the setup of electrochemical deposition is illustrated in Figure 1. The deposition was performed with three-electrode configuration, where as can be seen in Figure 1, the working electrode (WE) is connected to one of the microelectrodes inside the microchannel, whereas the counter (CE) and reference electrodes (RF) were connected to the two wide microelectrodes inside the reservoir A. Solution of approximately 5 mM of each metal salt was used for performing the deposition process. The microchannel was filled with the depositing solution by loading a drop into to reservoir A followed by applying gentle vacuum to reservoir B. the process was conducted under a microscope to assure no existence for air pebbles. The electrochemical deposition was stimulated via applying square pulse potential between –1800 mV and 0 mV with a frequency of 2 Hz for various periods of time (Figure 1, Inset II). Fresh solution was pumped to the microchannel regularly at interval time of 1 min by applying the vacuum for less than two seconds at reservoir B.

3. RESULTS AND DISCUSSION

The microelectrodes were characterized using cyclic voltammetry in order to estimate their surface area.

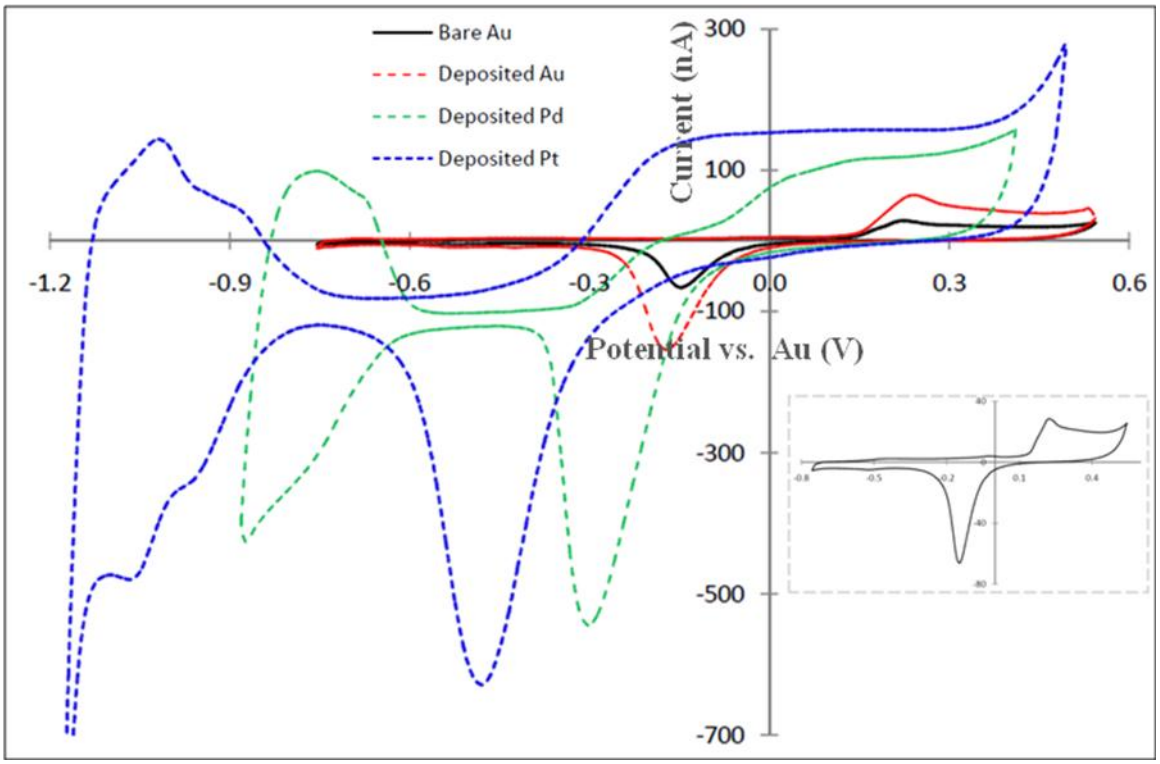

Figure 2. Cyclic Voltammograms of Au microelectrodes in 50 mM $HClO_4$ before and after modification with Au, Pd, and Pt nanoparticles. Inset: cyclic voltammogram of bare Au microelectrode. Scanning rate: 50 $mV.s^{-1}$.

Theoretically, the geometrical area of each microelectrode before modification is approximately 375 μm^2; however, the real surface area typically is larger than this because of surface roughness. Hence, real surface area for each microelectrode was estimated using the cyclic voltammogram of each microelectrode before and after modification obtained in 50 mM $HClO_4$. For gold micro electrodes, real surface area was estimated based on measuring the charge that corresponds to oxygen monolayer electrochemically deposited on the electrode surface; whereas real surface area of platinum and palladium microelectrodes was estimated by measuring the charge that corresponds to the electrochemically adsorbed monolayer of hydrogen on the surface of the microelectrode. It is noteworthy mentioning that the palladium and platinum microelectrodes were generated after electrochemical deposition of both metals on the surface of gold microelectrode. Figure 2 shows typical cyclic voltammograms obtained for the three metals after 8 min of deposition; the inset shows the cyclic voltammogram of bare gold microelectrode before modification. As can be noticed from Figure 2, typical cyclic voltammograms for gold, and platinum and palladium is obtained that are characterized with the oxygen deposition and hydrogen adsorption peaks, respectively. The cyclic

voltammograms are shifted toward lower potential, which can be attributed to the fact that potential was measured against the pseudo reference electrode, namely the gold microelectrode labeled as RE in Figure 1. However, such shift is insignificant in estimating the real area of the microelectrodes.

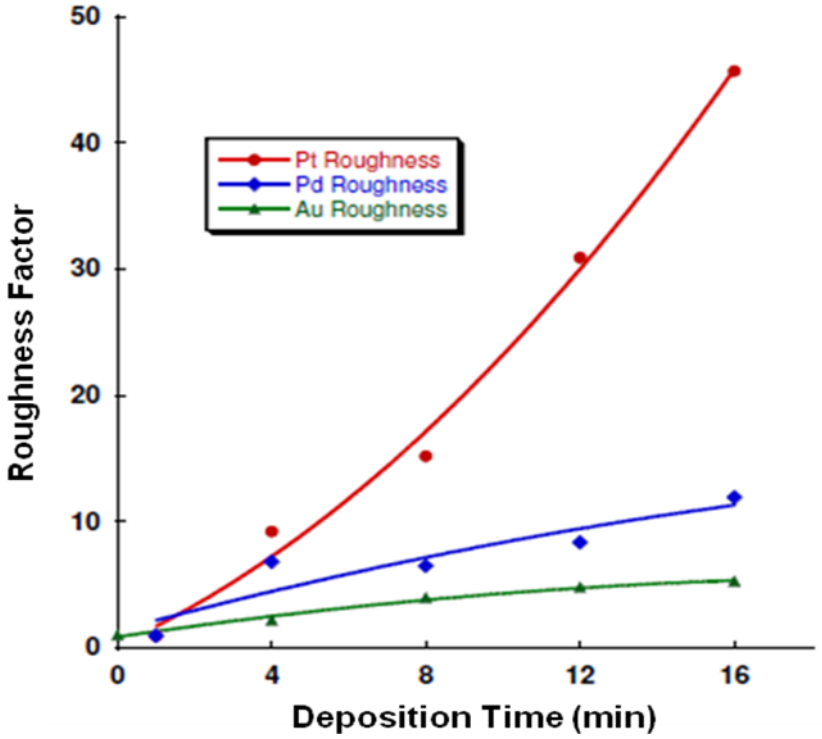

Figure 3. Roughness factor of Au, Pd, and Pt versus deposition time.

The electrochemical deposition was quantitatively analyzed based upon estimating the roughness factor of each microelectrode after the same period of deposition time. Hence, as depicted in Figure 2, platinum modified microelectrodes exhibited the largest roughness factor after 8 min of electrochemical deposition, where it approximately has one order of magnitude larger surface area than gold microelectrode. In addition, the roughness factor was estimated after various periods of deposition time in the range 0-16 min with the interval of 4 min. The first run for palladium and platinum was conducted after one min of deposition time. A plot of roughness factor of each metal versus deposition time is illustrated in Figure 3. Hence, an attempt has been performed to quantitatively correlate the roughness factor of each electrode with the deposition time, which in turn is represented by the trend lines as can be noticed in Figure 3.

Typically, increasing the roughness factor of working electrode is essential step in enhancing the sensitivity of the electrochemical measurements, which corresponds to enhancing the coulometric efficiency of the electrochemical sensors. The sensitivity of modified microelectrodes toward the neurotransmitter Dopamine was investigated via chronoamperometry. Figure 4 shows various results obtained for gold modified electrodes after deposition time in the range 0-16min; namely, roughness factor, height, and amperometric response to the neurotransmitter Dopamine. As can be noticed in

Figure 4, the roughness factor and amperometric response to dopamine reached their maximum values upon utilizing a microelectrode that has been modified with approximately 10 min of electrochemical deposition. Hence, this is consistent with the fact that roughness factor can be considered as an indication for the prospective sensitivity of the electrochemical sensors. In fact, regular increase in the height of the microelectrode was observed with increasing the deposition time, hence an increase in the roughness factor is expected, and consequently an enhanced amperometric response. However, we believe that this can be attributed to reduction in the size of the nanoparticles with increasing the deposition time. On the other hand, the height plot depicted in Figure 4 corresponds to height measurements made at the center of the electrodes.

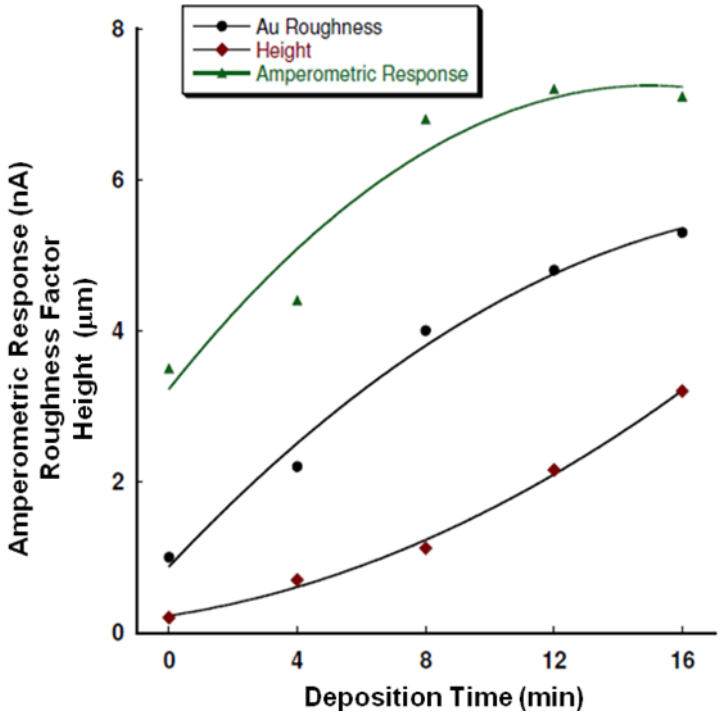

Figure 4. Amperometric signal of dopamine, roughness factor, and height of microelectrode versus deposition time of Au.

However, profilometric investigation revealed that modified microelectrodes exhibit irregular profile, where the height at the edges is notably higher that than at the center. Hence, we can anticipate that this profile of microelectrodes can induce generating unstable laminar or even turbulent flow around its territory [29], i.e. maintaining laminar regime is questioned , which reflects the observed results concerning the reduction in the stability of the amperometric background for long-time modified microelectrodes (data not shown). These observed profiles are illustrated in Figure 5. Such ledge effect can be attributed to the fact that in the process of electrochemical deposition of metals, existence of defects in the electrode surface is crucial in determining its final shape after electrochemical deposition for a period of time; this includes the regulatory in the electrode profile. In aqueous solutions, the metal ions are hydrated $[M(H_2O)_x]^{n+}$, where upon stimulating the

electrochemical deposition, they will transfer to their final state of M adatom on the electrode surface. Typically, this transition occurs via either Step-Edge Ion-Transfer Mechanism, or Terrace Ion-Transfer Mechanism.

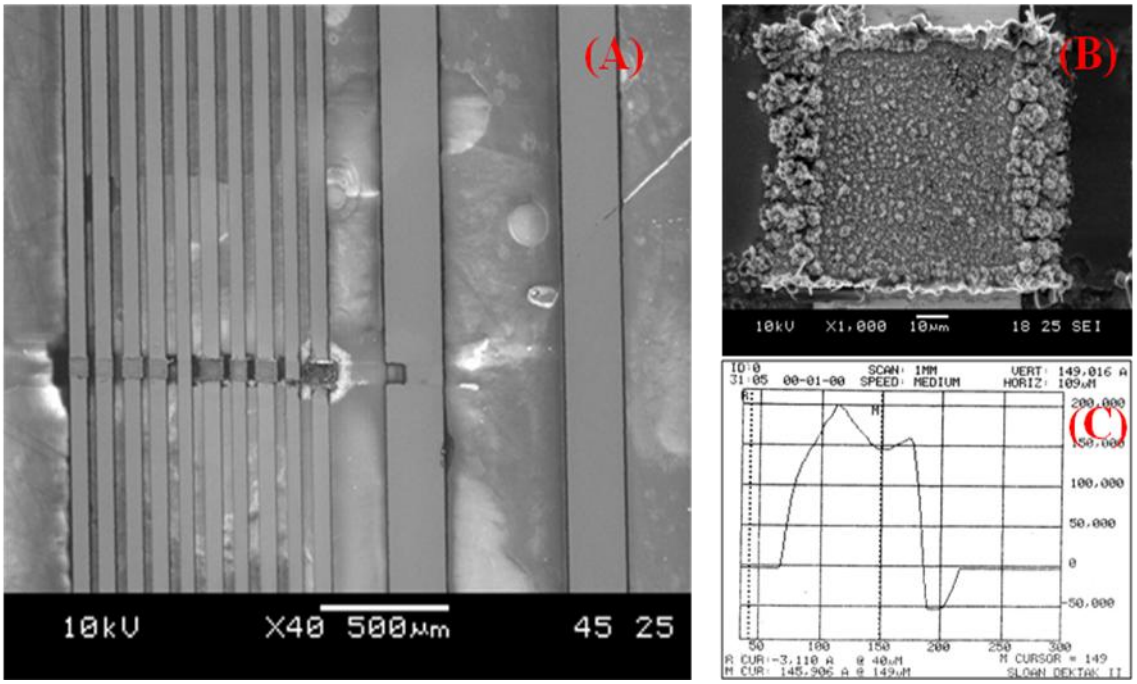

Figure 5. (A) SEM image for the microfluidic channel at the microelectrodes array region after modification, (B) SEM image and (C) Surface profilogram of a microelectrode after 30 min of electrochemical deposition of Au.

The main difference between them is the place where the adatom is located on the surface [40]. Hence, the former mechanism is favored in the presence of kinks, although the adatom will eventually end up at the same kink site via the latter mechanism. As mentioned earlier, the microelectrodes have a height of approximately 21nm at the edge before modification, which could trigger the edge effect upon performing the electrochemical deposition. Hence, regardless of which mechanism via which the adatom will proceed to the surface, the adatom will seek a position with lower potential energy, which is favorably at the edge of the microelectrode. These mechanisms potentially account for the observed edgy profile observed for microelectrodes modified with electrochemical deposition in microfluidic channel as can be seen in Figure 5-B.

4. CONCLUSIONS

In this work, we have further investigated the electrochemical deposition of various metals, namely gold, palladium and platinum over the surface of microelectrodes inside a microfluidic channel. Utilizing a variety of characterization methods, namely cyclic voltammetry, surface

profilometry, and scanning electron microscope (SEM) has successfully provided insights concerning the surface profile of the microelectrodes after various period of deposition time. On the other hand, the roughness factor of calculation indicated that a deposition time of 10 min was sufficient to reach the maximum possible sensitivity of the microelectrode upon performing chronoamperometric analysis for the neurotransmitter dopamine. Surface profilometry analysis has indicated that the microelectrode starts to exhibit a v-shape after sufficient time of electrochemical deposition, where the height of the microelectrode was approximately 30% more than that at the middle of the microelectrode. Hence these observations have been linked to the fitting mechanism of electrochemical deposition. We believe that our findings reported herein are of particular importance toward developing more sensitive electrochemical sensors as well as providing valuable insights regarding fluid flow inside a microfluidic channel retarded by a step in the middle of the microchannel.

Acknowledgement

This work was supported in part by a grant from the Strategic Research Unit at Taibah University (Nanotechnology Program Project Grant 08-NANO-22-05). The author is grateful to Dr. Elham Mohammad at Taibah Universuty, Prof. R.Jankowiak at Kansas State University (KS, USA), and Dr. T. Kawaguchi at Hokaido University (Japan) for their valuable discussion and support.

References

1. A.Manz, N. Grabner and H.M. Widmer, *Sens. Actuat*. 1 (1990) 244.
2. A.Manz, D.J. Harrison, J.C. Rettinger, E. Verpoorte, H. Ludi and H.M. Widmer, Transducers 91, *Digest of Technical Papers*, IEEE 91 CH2817 (1990) 939.
3. A.Arora, G. Simone, G.B. Salieb-Beugelaar, J.T. Kim and A. Manz, *Anal. Chem*. 82 (2010) 4830.
4. A.Lenshof A. Ahmad-Tajudin, K. Jaras, A.M. Sward-Nilsson, L. Aberg, G. Marko-Varga, J. Malm and H. Lilja, *Anal. Chem.* 81 (2009) 6030.
5. E. Sollier, M. Cubizolles, Y. Fouillet and J.L.A. Achard, *Biomed. Microdev.* 12 (2010) 485.
6. N.J. Munro, K. Snow, J.A. Kant and J.P. Landers, *Clin. Chem*. 45 (1999) 1906.
7. E.P. Kartalov, D.H. Lin, D.T. Lee, W.F. Anderson, C.R. Taylor and A.A. Scherer, *Electrophoresis* 29 (2008) 5010.
8. A.A. Dawoud, H. Saryia and I.M. Lazar, *Electrophoresis* 28 (2007) 4645.
9. D.L. House C.H. Chon, C.B. Creech, E.P. Skaar and D.Q. Li, *J. Biotechn.* 146 (2010) 93.
10. J.M. Armenta, A.A. Dawoud and I.M. Lazar, *Electrophoresis* 30 (2009) 1145.
11. D.S. Lee, SH. Park, K.H. Chung and H.B. Pyo *IEEE Sensors J.* 8 (2008) 558.
12. N. Ramalingam, Z. Rui, H.B. Liu, C.C. Dai, R. Kaushik, B. Ratnaharika and H.Q. Gong *Sens. Actuat.* B Chem. 145 (2010) 543
13. J.H. Sung, C. Kam and M.L. Shuler Lab Chip 10 (2010) 446.
14. Y. Wen and S.T. Yang, *Drug Discov*. 3 (2008) 1323
15. X. Li, J. Huang, G.F. Tibbits and P.C.H. Li, *Electrophoresis* 28 (2007) 4723.
16. S.L. Shen, Y. Li and S.A. Wakida, *Environ. Monit Assess*. 166 (2010) 573.
17. G. Chen, Y. Lin and J. Wang, *Talanta* 68 (2006) 497.
18. S. Wakida, K. Fujimoto, H. Nagai, T. Miyado, Y. Shibutani and S. Takeda, *J. Chromatogr*. A 1109 (2006) 179.
19. T. Masadome, K. Nakamura, D. Iijima, O. Horiuchi, B. Tossanaitada, S. Wakida and T. Imato, *Anal. Sciences* 26 (2010) 417.

20. A.A. Dawoud, T. Kawaguchi and R. Jankowiak *Anal. Bioanal. Chem*. 388 (2007) 245.
21. J. Friend and L. Yeo, 4 (2010) 026502.
22. B.V. Chikkaveeraiah, H. Liu, V. Mani, F. Papadimitrakopoulos and J.F. Rusling, *Electrochem. Commun*. 11 (2009) 819.
23. A.Daridon, M. Sequeira, G. Pennarun-Thomas, H. Dirac, J.P. Krog, P. Gravesen, J. Lichtenberg, D. Diamond, E. Verpoorte and N.F. de Rooij, *Sens. Actuators B Chem* 76 (2001) 235.
24. A.Berduquea, J. O'Briena, J. Aldermana and D.W.M. Arrigan, *Electrochem. Commun*. 10 (2008) 20.
25. X. Zhang, T. Wang, D. Zheng, J. Zhang , Y. Zhang, L. Zhu, C. Chen, J. Yan, H. Liu, Y. Lou, X. Li, B. Xia, *Int. J. Electrochem. Sci.* 2 (2007) 618.
26. P. Vulto, T. Huesgen, B. Albrecht and G.A. Urban, *J. Micromech. Microeng*. 19 (2009) 077001.
27. Vilares R, Hunter C, Ugarte I, Aranburu I, Berganzo J, Elizalde J, Fernandez LJ. *Sens Actuat* B Chem 147 (2010) 411.
28. Y. Henry, A. Fragoso, V. Beni, N. Laboria, J.L.A. Sánchez, D. Latta, F.V. Germar, K. Drese, I. Katakis and C.K. O'Sullivan, *Electrophoresis* 30 (2009) 3398.
29. J. Urbanski, J.A. Levitan, D.N. Burch, T. Thorsen and M.Z. Bazant, *J. Colloid Interf. Sci*. 309 (2007) 332.
30. B.J. Polk, A. Stelzenmuller, G. Mijares, W. MacCrehanb and M. Gaitan, *Sens. Actuat. B Chem* 114 (2006) 239.
31. L.P. Bicelli, B. Bozzini, C. Mele, L. D'Urzo, *Int. J. Electrochem. Sci.* 3 (2008) 356.
32. F.W. Campbell, R.G. Compton, *Int. J. Electrochem. Sci.* 5 (2010) 407.
33. A.A. Dawoud, T. Kawaguchi, Y. Markushin, M.D. Porter and R. Jankowiak, *Sens. Actuat. B Chem* 120 (2006) 42.
34. A.A.D. Bani-Yaseen, *IEEE Sensors J*. 9 (2009) 81.
35. A.A. Dawoud, T. Kawaguchi and R. Jankowiak, *Electrochem. Comm*. 9 (2007) 1536.
36. A.Wlasenko, F. Soltani, D. Zakopcan, D. Sinton and G.M. Steeves, *Phys. Rev*. E 81 (2010) 021601.
37. P. Shi and P.W. Bohn, *ACS Nano* 4 (2010) 2946. .
38. X.J. Huang, A.M. O'Mahony and R.G. Compton, *Small* 5 (2009) 776.
39. Q. Buali, L.E. Johms and R. Narayanan, *J. Appl. Math*. 71 (2006) 692.
40. M. Paunovic, M. Schlesinger, Fundamentals of Electrochemical Deposition, 2nd ed, John Wiley & Sons, Hoboken, NJ (2006).